Mineralogy and Petrology (2006) 88: 381–405
DOI 10.1007/s00710-006-0160-6

Mineralogy and Petrology
Printed in Austria

Evidence for diamond-grade ultra-high pressure metamorphism and fluid interaction in the Svartberget Fe–Ti garnet peridotite–websterite body, Western Gneiss Region, Norway

J. C. Vrijmoed[1,*], **H. L. M. Van Roermund**[2], and **G. R. Davies**[1]

[1] Petrology Department, Faculty of Earth and Life Science, Free University Amsterdam, Amsterdam, the Netherlands
[2] Structural Geology Group, Faculty of Earth Sciences, Utrecht University, Utrecht, the Netherlands
[*] Present address: Physics of Geological Processes, University of Oslo, Oslo, Norway

Received September 22, 2005; accepted March 28, 2006
Published online August 22, 2006;
Editorial handling: A. Mogessie

Summary

Based on mineral-chemical evidence we propose that the northernmost Scandian ultra-high pressure (UHP) metamorphic domain within the Western Gneiss Region of Norway can be extended 25 km northeastwards. A newly discovered, well preserved, fine-grained, Fe–Ti type garnet peridotite body at Svartberget, located in the Ulla Gneiss of the 'Møre og Romsdal' area north of Molde, is cut by a network of systematically orientated coarse-grained garnet-websterite and garnetite veins. Standard thermobarometric techniques based on electron microprobe analyses yield pressure (P) and temperature (T) estimates around 3.4 GPa, and 800 °C for the peridotite body and 5.5 GPa, and 800 °C for the websterite veins consistent with UHP conditions. In addition, polyphase solid inclusions, consisting of silicates, carbonates, sulphates and elemental carbon (including microdiamond), are randomly located in garnet and clinopyroxene of the websterite vein assemblage. Garnet-clinopyroxene mineral pairs yield a Sm–Nd cooling age of 393 ± 3 Ma for the peridotite and 381 ± 6 Ma for the vein assemblage suggesting that the Svartberget body was overprinted during the UHPM of the Scandian Orogeny. The initial ratio of the mineral isochron and Nd model ages suggest a mid-Proterozoic origin for the peridotite body. The polyphase inclusions, coupled with high $^{87}Sr/^{86}Sr$ ratios may indicate that the

peridotite body was infiltrated by crustal-derived C–O–H melts/fluids at UHPM conditions to form the websterite veins in the diamond field. We propose that fracturing and vein emplacement were the result of local high fluid pressure during subduction of the Baltic plate.

Introduction

The Western Gneiss Region (WGR) (Fig. 1) of SW-Norway consists of Proterozoic basement gneisses, remobilised in the Caledonian, that are interpreted to represent the outermost western part of the Baltic plate and overlying allochthonous units that have been correlated with the Caledonian nappes in northern and central Scandinavia (*Krill*, 1985; *Bryhni*, 1989; *Robinson*, 1995). The coastal part of the WGR (Fig. 1) is characterized by the occurrence of ultra-high pressure metamorphic (UHPM) rocks. Evidence for UHPM comes from the discovery of coesite and micro-diamond in peridotite, eclogite and kyanite-garnet gneiss (*Smith*, 1984; *Dobrzhinetskaya* et al., 1995; *Van Roermund* et al., 2002) and/or from the application of standard geothermobarometric techniques (*Terry* et al., 2000). Three distinct UHPM domains have previously been recognised (*Root* et al., 2005) (Fig. 1). In this paper we will focus on the size and magnitude of the northernmost UHPM terrane, initially discovered by *Dobrzhinetskaya* et al. (1995) and following vigorous debate, subsequently confirmed by *Terry* et al. (2000) and *Van Roermund* et al. (2002). Lateral eastwards and southwards expansions of the northernmost UHPM terrane towards, and across the islands of Otrøy and Fjørtoft were recently reported (*Van Straaten* et al., 2003; *Van Roermund* et al., 2005; *Carswell* et al., 2006). During the summers of 2003 and 2004, we performed a detailed field study/mapping project along the continuously exposed western coastline between Bud and Tornes (north of Molde; Figs. 1 and 2). This study reports the discovery of a well preserved Fe–Ti type garnet peridotite body, named Svartberget, exposed within felsic gneisses of the WGR (*Carswell* and *Harvey*, 1982). The felsic gneisses are often migmatitic and have tonalitic to dioritic compositions. This gneiss unit is recognised in neighbouring areas (e.g. Fjørtoft, Otrøy) as the Ulla Gneiss (*Terry* and *Robinson*, 2003). We present electron microprobe (EMP) mineral analyses and use standard geothermobarometric techniques and mineralogy to demonstrate that the Svartberget body has been metamorphosed within the UHPM field indicating that the northernmost UHP domain extends more than 25 km further northeastwards than previously recognised (Fig. 1). In addition, we report isotope geochemical data that give strong indications for

Fig. 1. Overview of the Western Gneiss Region (WGR) and overlying Caledonian thrust nappes in the surrounding area. The three distinct UHP domains within the WGR are shaded. Numbers indicate the following garnet peridotite localities: Fe–Ti type: *1* Eiksunddalen; *2* Raknestangen; *3* Kolmannskog; *4* Lyngenes; *10* Svartberget. Mg–Cr type: *5* Almklovsdalen; *6* Kalskaret; *7* Ugelvik; *8* Sandvik; *9* Raudhaugene (from *Carswell* et al. (1983)). The temperature gradients are shown (after *Krogh* (1977)). The Figure is compiled after data from *Krogh* (1977), *Bryhni* and *Sturt* (1985), *Griffin* et al. (1985), *Robinson* (1995), *Root* et al. (2005)

fluid infiltration of the Svartberget peridotite, and we investigate the original intrusion and subsequent metamorphic age of the Svartberget Fe–Ti peridotite body.

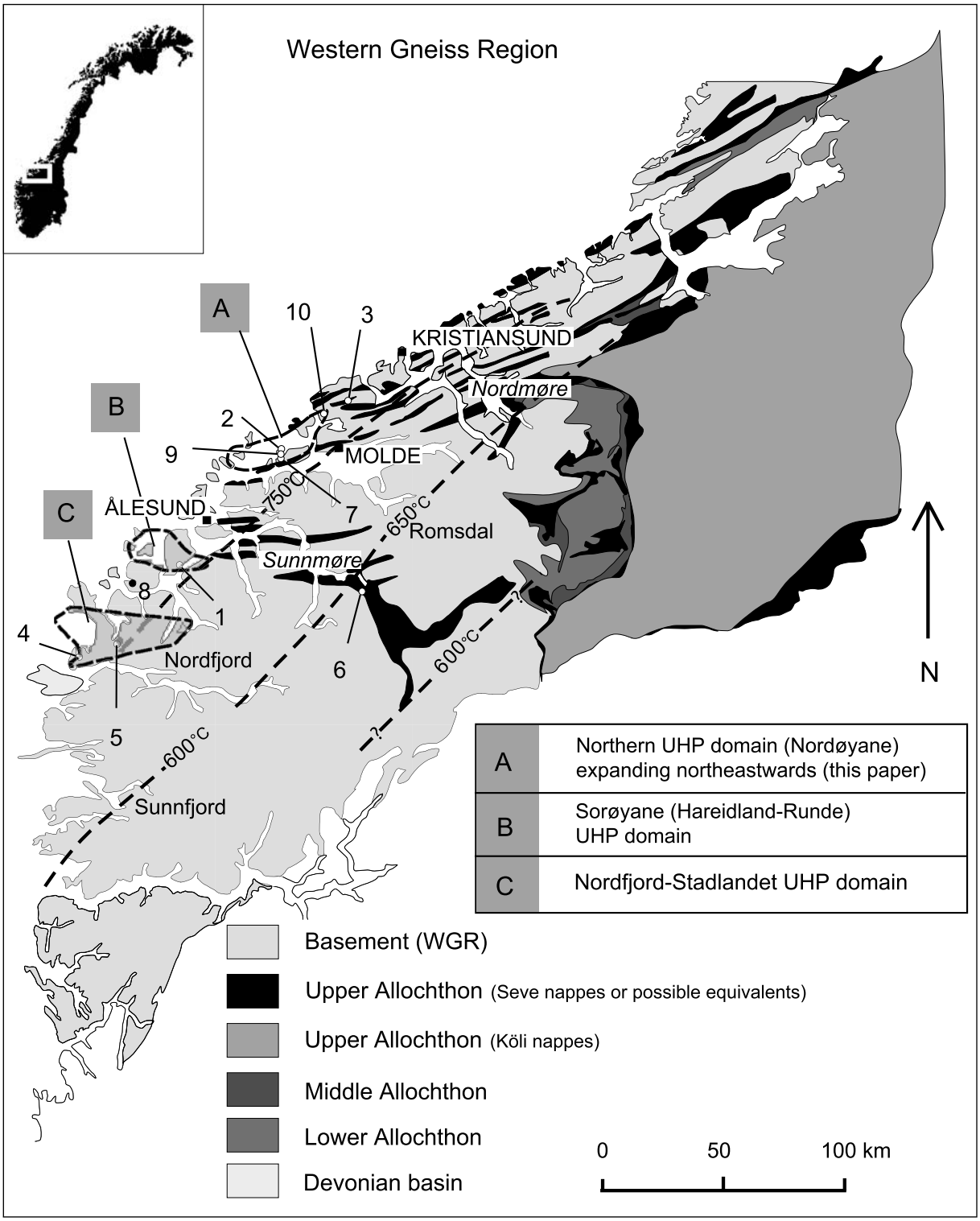

Regional geology

The large-scale structure and geology of the WGR and surrounding areas are presented in Fig. 1. The WGR is a reworked large Caledonian basement window, presumably connected to the Baltic plate in the east (*Cuthbert* et al., 2000). During the Caledonian Orogeny the Iapetus Ocean closed (*Torsvik* et al., 1996) and oceanic fragments, island arcs, micro-continents, imbricated basement slivers and overlying late Proterozoic-early Paleozoic sediments were thrust, from west to east, over the basement/Baltic plate as nappes (*Roberts*, 2003; *Brueckner* and *Van Roermund*, 2004). Post-dating regional nappe transport, Baltica subducted to UHP conditions during the latest part of the Scandian Orogeny (*Hacker* et al., 2001; *Carswell* et al., 2003b). The overlying supracrustal nappes can now be found to the north, east and south of the WGR, underneath the Devonian basins in the west and at isolated, scattered, areas throughout the WGR.

The Bud-Tornes area

Post-dating the Scandian UHPM, the rocks of the WGR were strongly folded at the macro-scale (km) resulting in a NE–SW trending structural pattern in which the Caledonian nappes can be traced in dominantly syn – but also anti-formal structures with subvertical axial planes (*Krill*, 1985; *Robinson*, 1995; *Krabbendam* and *Dewey*, 1998). These folds are interpreted to be related to the exhumation of the UHPM terrane (*Seranne*, 1992; *Andersen*, 1998; *Krabbendam* and *Dewey*, 1998). Whether the folds are synchronous or actually post-date exhumation is still debated, but they were formed in rocks that were at amphibolite facies conditions. Two of these, apparent synclinal, folds are exposed in the studied area and involve possible Caledonian nappes and Proterozoic basement elements (*Robinson*, 1995; *Tveten* et al., 1998). Our structural and lithological analysis of these NE–SW trending supracrustal ''synforms'' revealed that the investigated structures are much more complicated than previously mapped (*Tveten* et al., 1998). We found no evidence that was consistent with a synformal character. The detailed geological map, illustrated in Fig. 2, is a simplified version of our field-map, which displayed too many individual lithological units to be reproduced here. Individual units were grouped into major units on the basis of field characteristics and rock type to form Fig. 2. All units are strongly deformed and often mylonitic. The major lithological units in Fig. 2 are:

1) *Tonalitic-dioritic gneiss and migmatites.* This unit is referred to as Ulla Gneiss in neighbouring areas, shows transpositional folds in many places and variable degrees of migmatisation and strain/mylonitisation. The unit contains abundant eclogites, amphibolites and some gabbros.
2) *Tonalitic gneiss with sillimanite and/or white mica*. This unit occurs within unit (1) described above. Garnet is present locally and in some places the dominant rock type is schist, especially where white mica is more abundant.
3) *Fine-grained tonalitic gneiss.* This unit displays strong deformation in localised shear zones. Abundant feldspar (often <0.5 cm in size), and subordinate garnet porphyroclasts are present.
4) *Garnet-biotite schist, amphibolite and marble.* Different rock units alternate on a scale of several decimeters to meters. The schist contains 1–2 cm sized garnet

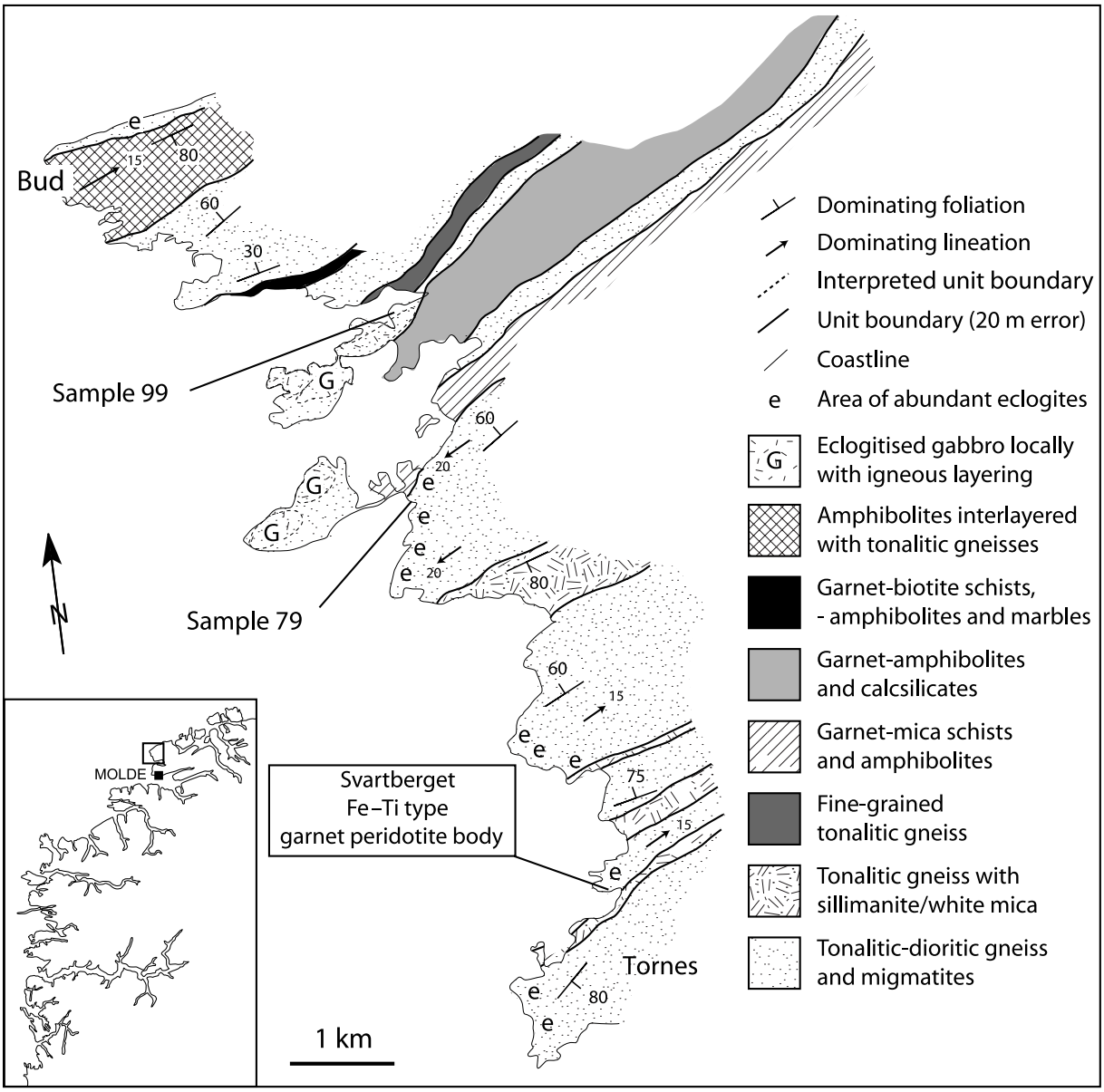

Fig. 2. Geological map of the Tornes-Bud area

porphyroclasts, abundant biotite, plagioclase and amphibole. The amphibolite consists of amphibole, plagioclase and in some layers abundant garnet porphyroclasts. Marble was found as single layers with a maximum thickness of 20–30 cm.

5) *Garnet-amphibolite and calcsilicate.* Dominantly layered amphibolites with plagioclase, biotite and abundant garnet porphyroclasts. Minor amounts of foliated biotite-rich amphibolites and single calcsilicate layers (10–20 cm thick).
6) *Amphibolite interlayered with tonalitic gneiss and garnet-biotite schist.* Amphibolitic bands alternating with quartzo-feldspathic gneiss bands and rusty

weathered garnet-biotite schists. Some amphibolite layers contain abundant garnet porphyroclasts.

7) *Garnet-mica schists and amphibolites*. Layered unit consisting dominantly of mylonitic garnet mica-schist, and garnet amphibolite, and subordinate fine grained biotite-plagioclase-quartz gneiss up to several meters thick.

Previous workers have mapped this and neighbouring regions (*Carswell* and *Harvey*, 1982; *Mørk*, 1985b; *Bryhni* et al., 1989; *Robinson*, 1995; *Terry* et al., 2000) and a 1:250,000 geological map was recently published (*Tveten* et al., 1998). In general the divisions made to form our field units (see Fig. 2) are in agreement with those of *Bryhni* et al. (1989). In this area no correlation can be made with the mid-Proterozoic augen gneiss units found northwest of Molde and on Otrøy (*Carswell* and *Harvey*, 1982). Our tonalitic-dioritic gneiss and migmatite (unit 1), Ulla Gneiss, correlates with the undifferentiated paragneiss unit of *Carswell* and *Harvey* (1982) and *Harvey* (1983) and the Baltica basement described by *Robinson* (1995). *Bryhni* et al. (1989) describe this unit as undifferentiated, usually migmatitic gneiss of Precambrian age, named the Valsøyfjorden Complex. The tonalitic gneiss with sillimanite/white mica (unit 2) also correlates to the Valsøyfjorden Complex of *Bryhni* et al. (1989). All other units are equivalent to the metamorphosed supra-crustal rocks from the Ertvågøy Group (*Bryhni* et al., 1989). Our garnet-biotite schist, amphibolite and marble unit (unit 7) may be correlated to the Blåhø-Surna Nappe of *Robinson* (1995). Our experience, however, is that regional correlation between individual units remains difficult. Possible thrust contacts between individual units are unrecognisable because the area is dominantly a high-strain/mylonite zone.

The Svartberget Fe–Ti type garnet peridotite/websterite body

Garnet peridotites in the WGR have been divided into Mg–Cr and Fe–Ti type (*Carswell* et al., 1983; *Krogh* and *Carswell*, 1995). The Mg–Cr type garnet peridotites have upper mantle affinities; whereas the Fe–Ti type garnet peridotites form most likely in the mid-Proterozoic as lower crustal cumulates of layered mafic igneous intrusions (*Schmidt*, 1963; *Mørk*, 1985a, b; *Jamtveit*, 1987a, b). They are called Fe–Ti type because: 1) the bulk chemistry is high in iron (Fo $\sim$ 70–80) and 2) the rocks contain 1–5 modal% Fe–Ti oxides and green spinels (*Carswell* et al., 1983). In Fig. 1 it can be seen that the Svartberget garnet peridotite body lies along strike with other known occurrences of Fe–Ti type peridotite (Raknestangen, nr. 2 on the island Otrøy and Kollmanskog, nr. 3 north of Molde). The Svartberget Fe–Ti type garnet peridotite body (1600 m^2) has been mapped in detail (Fig. 3).

Figure 3 shows that the peridotite body has undergone extensive fracturing prior to, or associated with the emplacement of garnet-bearing websterites, that are variable in their modal abundance and distribution of garnet and pyroxene, and that are strongly associated with garnetites ('garnetite-websterite veins', Fig. 3). The websterite veins associated with garnetite and the garnetite form a unit that define a network with pronounced preferred orientations (poles to the planes: $\sim$260/10 and $\sim$200/10, Fig. 3b) that cut the peridotite into individual blocks that range in area from 1 to 10 m^2.

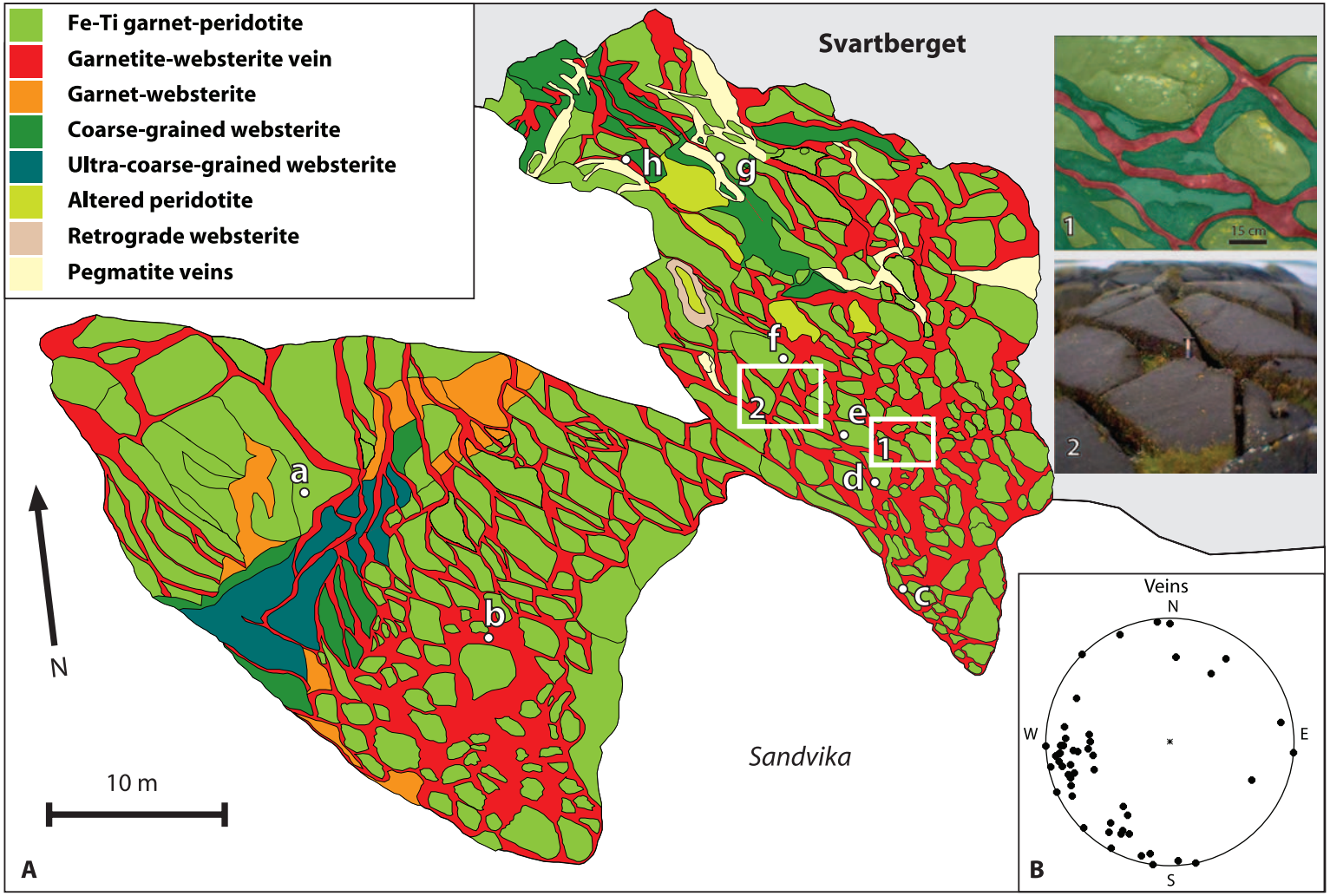

Fig. 3. (a) Detailed map of the Svartberget Fe–Ti type garnet peridotite body (see text for further explanation). Samples taken for Sm–Nd isotope analysis are: a = 04–31; b = 04–33; c = 04–38; d = 04–37; e = 8; f = 04–2; g = 7; h = 6. Rectangles show location of inset Figs. 1 and 2. Inset 1 is an annotated field picture showing how the red coloured unit in the map, indicated in the legend by 'garnet-websterite veins', looks in more detail. Colours in inset 1: green = garnet-peridotite, dark-green = garnet-websterite, red = garnetite. Inset 2 shows the preferred orientation of the veins. (b) Stereographic projection (lower hemisphere) of poles to the planes from measured veins ($n = 50$) establishing the preferred orientation of the veins seen in Fig. a

In regions where websterite is strongly associated with garnetite (e.g. 'garnetite-websterite veins' in Fig. 3), the garnet-bearing websterite veins are themselves cut by garnetite. The garnetite can form layers up to 10 cm thick, and is usually found in the cores of the websterites, but it can also form pods or complex networks of smaller veins that cross-cut the websterites. Thick garnetite veins may have a core of phlogopite (<0.5 cm thick). In the south-western part of the body cross-cutting relationships indicate that coarse-grained to ultra-coarse grained garnet websterite occurs in a zone that is relatively older than the websterites cored by garnetites (Fig. 3). Post eclogite facies pegmatites occur in the northern part of the body. Locally some of the peridotite blocks are heavily altered or retrogressed.

The peridotite body consists of (<1 mm) garnet, clinopyroxene, orthopyroxene, olivine and ~1–5 modal% Fe–Ti oxides. The modal olivine (Fo = 83) content varies between 20 and 30%, where approximately 5–10% is serpentinised. Cross-cutting garnet-bearing websterite consists of (~1–5 mm) clinopyroxene, orthopyroxene, garnet and phlogopite (and very minor secondary amphibole). The garnetite veins generally consist of garnet and phlogopite. (Ultra) coarse grained websterite consists of orthopyroxene, clinopyroxene, garnet and phlogopite with grain sizes ranging between 2 and 5 cm (coarse grained) up to 20 cm (ultra coarse grained). Figure 3 (insets 1 and 2) illustrates some of the general structural relationships between the main body and garnet websterite and garnetite veins.

Methods and techniques

Electron microscopy was performed at the Electron Microscopy and Structure Analyses Centre, Utrecht University. EMP analyses were performed with the JEOL JXA-8600 Superprobe at Utrecht University. Operating conditions were 15 KV accelerating voltage and a beam current of 20 nA. Line-scans were made across all single grains to check for chemical-heterogeneity. Peak pressures (P) and temperatures (T) were estimated using the aluminium in orthopyroxene (in the presence of garnet) barometers $P_{H\&G82}$ (*Harley* and *Green*, 1982), P_{H84}, (*Harley*, 1984b), $P_{N\&G85}$ (*Nickel* and *Green*, 1985) and $P_{B\&K1990}$ (*Brey* and *Köhler*, 1990) in combination with the garnet-orthopyroxene Fe–Mg exchange thermometers T_{H84} (*Harley*, 1984a), $T_{L\&G88}$, (*Lee* and *Ganguly*, 1988), $T_{L\&G88}$ using $W_{Ca} = 1500$ (*Carswell* and *Harley*, 1990), $T_{B\&K90}$ (*Brey* and *Köhler*, 1990), and garnet-clinopyroxene Fe–Mg exchange thermometers $T_{R\&G74}$, (*Råheim* and *Green*, 1974), $T_{E\&G79}$ (*Ellis* and *Green*, 1979), T_{P85} (*Powell*, 1985), T_{K88} (*Krogh*, 1988), T_{R2000} (*Ravna*, 2000), two pyroxene thermometers T_{W77} (*Wells*, 1977) and $T_{B\&K90}$ (*Brey* and *Köhler*, 1990), the calcium in orthopyroxene and sodium in orthopyroxene thermometers $T_{B\&K90Ca}$ and $T_{B\&K90Na}$ (*Brey* and *Köhler*, 1990), respectively, and the garnet-olivine Fe–Mg thermometer $T_{O\&W79}$ (*O'Neill* and *Wood*, 1979) including the correction term of *O'Neill* (1980). Where used, ferric iron in clinopyroxene is estimated using the method of *Droop* (1987). Representative EMP analyses and P–T estimates of selected minerals are presented in Tables 1 and 2, respectively.

Isotopic analyses were performed on a Finnigan Mat 262 RPQ plus thermal ionisation mass spectrometer (TIMS) at the Vrije Universiteit, Amsterdam,

Table 1. *Representative electron microprobe analyses of selected minerals from a specimen of the garnet peridotite body (sample 8) and a cross-cutting garnet websterite vein (sample 6)*

Locality:	Svartberget				Garnet websterite vein		
Sample:	Main body						
Mineral:	Grt	Cpx	Opx	Ol	Grt	Cpx	Opx
Line no.:	8-4a	8-4b	8-4c	8-4d	6-20f	6-20d	6-20d
Spot:	core	core	core	core	core	core	core
SiO_2	41.46	55.18	57.40	39.93	40.88	54.70	57.17
TiO_2	0.01	0.00	0.02	–	0.03	0.01	0.00
Al_2O_3	21.97	0.51	0.51	–	21.84	1.14	0.16
Cr_2O_3	0.50	0.09	0.01	0.00	0.39	0.19	0.03
FeO	14.66	2.98	10.23	15.82	18.12	4.67	11.78
Fe_2O_3	–	–	–	–	–	–	–
MnO	0.87	0.09	0.19	0.26	0.86	0.10	0.18
MgO	15.73	17.38	32.39	44.60	14.53	15.88	31.16
CaO	5.25	23.86	0.17	0.00	4.11	22.00	0.18
Na_2O	0.01	0.44	0.01	–	0.01	1.07	0.00
NiO	–	–	–	0.25	–	–	–
Total	100.47	100.54	100.94	100.87	100.77	99.76	100.65
Py	55.73	–	–	–	51.63	–	–
Alm	29.14	–	–	–	36.13	–	–
Gr	13.37	–	–	–	10.51	–	–
Sps	1.76	–	–	–	1.73	–	–
Wo	–	47.37	0.31	–	–	46.08	0.35
En	–	48.02	84.68	–	–	46.30	82.20
Fs	–	4.61	15.01	–	–	7.62	17.45
Jd	–	0.92	–	–	–	2.58	–
Ac	–	1.01	–	–	–	1.21	–
Di + Hed	–	97.54	–	–	–	93.63	–
Fo	–	–	–	83.40	–	–	–
Fa	–	–	–	16.60	–	–	–
Cations							
Si	3.03	2.00	1.99	1.00	3.01	2.00	2.00
Ti	0.00	0.00	0.00	–	0.00	0.00	0.00
Al	1.89	0.02	0.02	–	1.90	0.05	0.01
Cr	0.03	0.00	0.00	0.00	0.02	0.01	0.00
Fe(II)	0.89	0.07	0.30	0.33	1.12	0.12	0.35
Fe(III)		0.02	0.00	–	–	0.02	0.00
Mn	0.05	0.00	0.01	0.01	0.05	0.00	0.01
Mg	1.71	0.94	1.68	1.66	1.60	0.87	1.63
Ca	0.41	0.92	0.01	0.00	0.32	0.86	0.01
Na	0.00	0.03	0.00	–	0.00	0.08	0.00
Ni	–	–	–	0.01	–	–	–
Total	8.02	4.01	4.00	4.00	8.03	4.01	3.99

the Netherlands, following techniques outlined in (*Griselin*, 2001; *Griselin* et al., 2001). An internal Nd standard yielded 0.51134 ± 0.00001, which equates to La Jolla of 0.51186, and NBS 987 Sr standard yielded 0.71028 ± 0.00001.

Table 2. *Representative P–T estimates for the garnet websterite vein (sample 6) and the garnet peridotite (sample 8). See text for further explanation and abbreviations*

Geothermobarometer		Fe^{3+} estimated		$Fe_{total} = Fe^{2+}$	
		T	*P*	*T*	*P*
Garnet websterite vein (sample 6)					
T_{H84}	$P_{B\&K1990}$	1000	7.1		
$T_{L\&G88}$	$P_{B\&K1990}$	1317	10.6		
$T_{L\&G88}$*	$P_{B\&K1990}$	1192	9.2		
$T_{B\&K90}$	$P_{B\&K1990}$	919	6.3		
$T_{R\&G74}$	$P_{B\&K1990}$	1585	11.8	1555	12.6
$T_{E\&G79}$	$P_{B\&K1990}$	939	6.5	849	5.6
T_{P85}	$P_{B\&K1990}$	899	6.1	810	5.3
T_{K88}	$P_{B\&K1990}$	794	5.1	701	4.3
T_{R2000}	$P_{B\&K1990}$	1019	7.3	821	5.4
T_{W77}	$P_{B\&K1990}$	829	5.5	838	5.5
$T_{B\&K90}$	$P_{B\&K1990}$	881	5.9	873	5.9
$T_{B\&K90Ca}$	$P_{B\&K1990}$	907	6.2		
$T_{B\&K90Na}$	$P_{B\&K1990}$	error	error		
Peridotite main body (sample 8)					
T_{H84}	$P_{B\&K1990}$	926	4.3		
$T_{L\&G88}$	$P_{B\&K1990}$	1178	6.4		
$T_{L\&G88}$*	$P_{B\&K1990}$	1068	5.5		
$T_{B\&K90}$	$P_{B\&K1990}$	847	3.7		
$T_{R\&G74}$	$P_{B\&K1990}$	976	4.7	854	3.8
$T_{E\&G79}$	$P_{B\&K1990}$	784	3.3	714	2.8
T_{P85}	$P_{B\&K1990}$	753	3.1	682	2.6
T_{K88}	$P_{B\&K1990}$	674	2.5	601	2.0
T_{R2000}	$P_{B\&K1990}$	632	2.3	539	1.7
T_{W77}	$P_{B\&K1990}$	808	3.5	814	3.5
$T_{B\&K90\text{-}2px}$	$P_{B\&K1990}$	732	2.9	729	2.9
$T_{B\&K90Ca}$	$P_{B\&K1990}$	779	3.3		
$T_{B\&K90Na}$	$P_{B\&K1990}$	895	4.1		
$T_{O\&W79}$	$P_{B\&K1990}$	794	3.4		

* $W_{Ca} = 1500$ (*Carswell* and *Harley*, 1990)

Sm–Nd isotope systematics are reported for 8 whole-rock samples (Table 3). The results of 2 garnet and 2 clinopyroxene separates from samples of the Svartberget body are given in Table 3. In addition minerals from surrounding ''country-rock'' eclogites (sample locations, see Fig. 2) were analysed (Table 3). Sample locations for the Svartberget body are given in Fig. 3a. Rb–Sr isotope systematics were determined on garnet and clinopyroxene mineral separates. The minerals were leached for 15 minutes in 1.0 N ultra-clean HCl in an ultrasonic bath. The same procedure was repeated using 1.4 N ultra-clean HNO_3.

The time of peak Scandian metamorphism in the region is estimated around 400 Ma (*Hacker* et al., 2001; *Carswell* et al., 2003a; *Krogh* et al., 2003), therefore all initial isotope ratios are reported for 400 Ma unless otherwise stated (Table 3),

Table 3. *Rb–Sr and Sm–Nd isotope data. All errors are 2σ. Errors of $^{147}Sm/^{144}Nd$ are 0.15%, based on repeated standard measurements by previous users at the Vrije Universiteit, Amsterdam. N.D. not determined. Initial Sr and Nd isotope ratios are calculated for minerals and whole rock samples at 400 Ma BP. Model age errors were propagated according to* Sambridge *and* Lambert *(1997)*

Sample	Min.	Sr (ppm)	Rb (ppm)	Rb/Sr	$^{87}Sr/^{86}Sr$	$^{87}Rb/^{86}Sr$	$^{87}Sr/^{86}Sr_i$	Nd (ppm)	Sm (ppm)	Sm/Nd	$^{147}Sm/^{144}Nd$	$^{143}Nd/^{144}Nd$	$^{143}Nd/^{144}Nd_i$	$\varepsilon_{CHUR}{}^0$	$\varepsilon_{CHUR}{}^t$	$T_{grt-cpx}$ (Ma)	T_{CHUR} (Ga)	T_{DM} (Ga)
Svartberget Fe–Ti peridotite/websterite body																		
Pyroxenite veins																		
6	grt	1.937	0.064	0.033	0.73865 ± 2	0.097	0.73811	0.506	1.075	2.127	1.287	0.51492 ± 4	0.51171 ± 2	44.5	−8.5 ± 0.5	380.7 ± 5.7	–	–
6	cpx	166.310	0.666	0.004	0.74257 ± 1	0.012	0.74251	10.478	2.634	0.251	0.152	0.51209 ± 2	0.51171 ± 2	−10.7	−8.5 ± 0.5		–	–
6	w.r.	–	–	–	–	–	–	3.837	1.174	0.306	0.185	0.51215 ± 1	0.51169 ± 2	−9.6	– ± 0.2	–	6.30 ± 0.29	5.22 ± 0.11
04–37	w.r.	–	–	–	–	–	–	8.100	2.257	0.279	0.168	0.51211 ± 1	0.51169 ± 1	−10.4	– ± 0.2	–	2.85 ± 0.08	3.44 ± 0.06
Garnitite vein																		
04–38	w.r.	–	–	–	–	–	–	3.416	1.781	0.521	0.315	0.51269 ± 1	0.51190 ± 1	0.9	– ± 0.1		0.06 ± 0.01	−0.70 ± 0.01
Perioditite/websterite blocks																		
8	grt	1.977	0.012	0.006	0.72309 ± 3	0.017	0.72299	0.760	1.100	1.448	0.876	0.51420 ± 1	0.51195 ± 1	30.5	−3.6 ± 0.2	393.4 ± 3.4	–	–
8	cpx	99.758	n.d.	n.d.	0.72702 ± 1	n.d.	n.d.	6.256	1.514	0.242	0.146	0.51233 ± 1	0.51195 ± 1	−6.1	−3.6 ± 0.2		–	–
8	w.r.	–	–	–	–	–	–	2.777	0.927	0.334	0.202	0.51238 ± 1	0.51186 ± 1	−5.0	– ± 0.3	–	−7.74 ± 0.85	9.55 ± 0.43
7	w.r.	–	–	–	–	–	–	2.869	0.883	0.308	0.186	0.51236 ± 1	0.51188 ± 1	−5.4	– ± 0.2	–	3.94 ± 0.23	4.27 ± 0.10
04–2	w.r.	–	–	–	–	–	–	2.111	0.605	0.287	0.173	0.51230 ± 1	0.51185 ± 1	−6.6	– ± 0.2	–	2.21 ± 0.08	3.15 ± 0.05
04–31	w.r.	–	–	–	–	–	–	4.605	1.144	0.248	0.150	0.51207 ± 1	0.51168 ± 1	−11.1	– ± 0.1	–	1.86 ± 0.03	2.56 ± 0.03
04–33	w.r.	–	–	–	–	–	–	4.241	1.205	0.284	0.172	0.51217 ± 1	0.51173 ± 1	−9.1	– ± 0.1	–	2.84 ± 0.08	3.53 ± 0.06
Country–rock eclogites																		
79	grt	2.131	0.080	0.038	0.71003 ± 3	0.109	0.70942	0.694	1.105	1.592	0.963	0.51425 ± 2	0.51176 ± 3	31.3	−7.2 ± 0.6	394.1 ± 6.2	–	–
79	cpx	176.536	0.090	0.001	0.70960 ± 1	0.001	0.70959	10.472	2.816	0.269	0.163	0.51218 ± 3	0.51176 ± 3	−9.0	−7.2 ± 0.6		–	–
99	grt	26.256	0.111	0.004	0.70296 ± 4	0.012	0.70289	1.745	2.856	1.637	0.990	0.51444 ± 1	0.51198 ± 3	35.2	−3.3 ± 0.5	380.1 ± 4.5	–	–
99	cpx	123.652	0.033	0.000	0.70523 ± 1	0.001	0.70522	17.272	5.553	0.321	0.194	0.51246 ± 2	0.51198 ± 3	−3.4	−3.3 ± 0.5		–	–

to allow assessment of the possible involvement of the continental crust in the formation of the peridotite-websterite body.

Results and discussion

Mineral chemistry

We obtained mineral-chemical data from well-preserved parts of thin sections from a garnet-websterite vein (sample 6) and the peridotite body (sample 8). Sample 6 consists of 1–5 mm sized crystals of diopsidic clinopyroxene ($Wo_{46}En_{46}Fs_{8,}$ Jd_4), orthopyroxene (En_{81-82}), garnet ($Pyr_{50-52}Alm_{35}Gross_{11-13}$) and phlogopitic biotite (Phl_{85}) (Fig. 4a). In contrast, the sample 8 is composed of smaller (<1 mm) diopsidic clinopyroxene ($Wo_{47}En_{48}Fs_5$, Jd_{1-2}), orthopyroxene ($En_{84-86,}$ Al_2O_3), garnet ($Pyr_{56}Alm_{29}Gross_{13}$) and olivine ($Fo_{83}$) (Fig. 4b). Profiles of the Al_2O_3 abundances across selected orthopyroxene grains from samples 6 and 8 are illustrated in Fig. 4. The bowl-shaped Al_2O_3 profiles suggest that diffusion processes were operating along grain margins, due to partial re-equilibration during retrogression (*Dodson*, 1973; *Ganguly* and *Tirone*, 1999). In contrast, garnet, clinopyroxene and olivine show constant composition profiles across the grains.

Polyphase solid inclusions

Polyphase solid inclusions were found inside garnet and clinopyroxene from garnet websterite and garnetite vein samples. The inclusions are not found in the garnet peridotite body itself. The assemblages comprise carbon, magnesite, dolomite, monazite, apatite, xenotime, titanite, pyrite, chalcopyrite, pentlandite, galena, Fe-oxides, orthite, gypsum, Ba-sulphates (+Sr), Ca-sulphate (+Sr), (unknown) W-, Al- and Al–Cl-silicates, Al–Fe–Mg-oxides, opx, cpx and grt (Fig. 6a and b). Similar inclusions were described by *Carswell* and *Van Roermund* (2005) from the Bardane peridotite on Fjørtoft. A micro-Raman spectroscopic study of some carbon grains, performed by D. C. Smith in Paris, verified the presence of micro-diamond (*Vrijmoed* et al., in prep.). The inclusions are irregularly shaped and randomly distributed within garnet but some also occur in clinopyroxene. Many of the minerals that define the polyphase solid inclusion assemblage are not included in the mineralogy of the main peridotite body or the websterite veins (e.g. monazite, magnesite, dolomite etc.) implying that (some and/or all) elements must have been introduced from outside the garnet peridotite body. From the major element chemistry of these silicate, carbonate, phosphate and sulphate inclusions, in combination with elemental carbon it can be concluded that immiscible silicate-carbonate-sulphate fluids (or melts) were involved in the formation of these polyphase inclusions. Carbon precipitated under reducing conditions and some carbon formed as micro-diamonds, indicating that crystallisation took place within the diamond UHPM field. At UHPM conditions these immiscible fluids/melts are probably well above the so called second critical point where there is no distinction between melt and fluid (*Stalder* et al., 2000; *Hermann*, 2003). Such fluids/melts were referred to by *Carswell* and *Van Roermund* (2005) as C–O–H rich fluids.

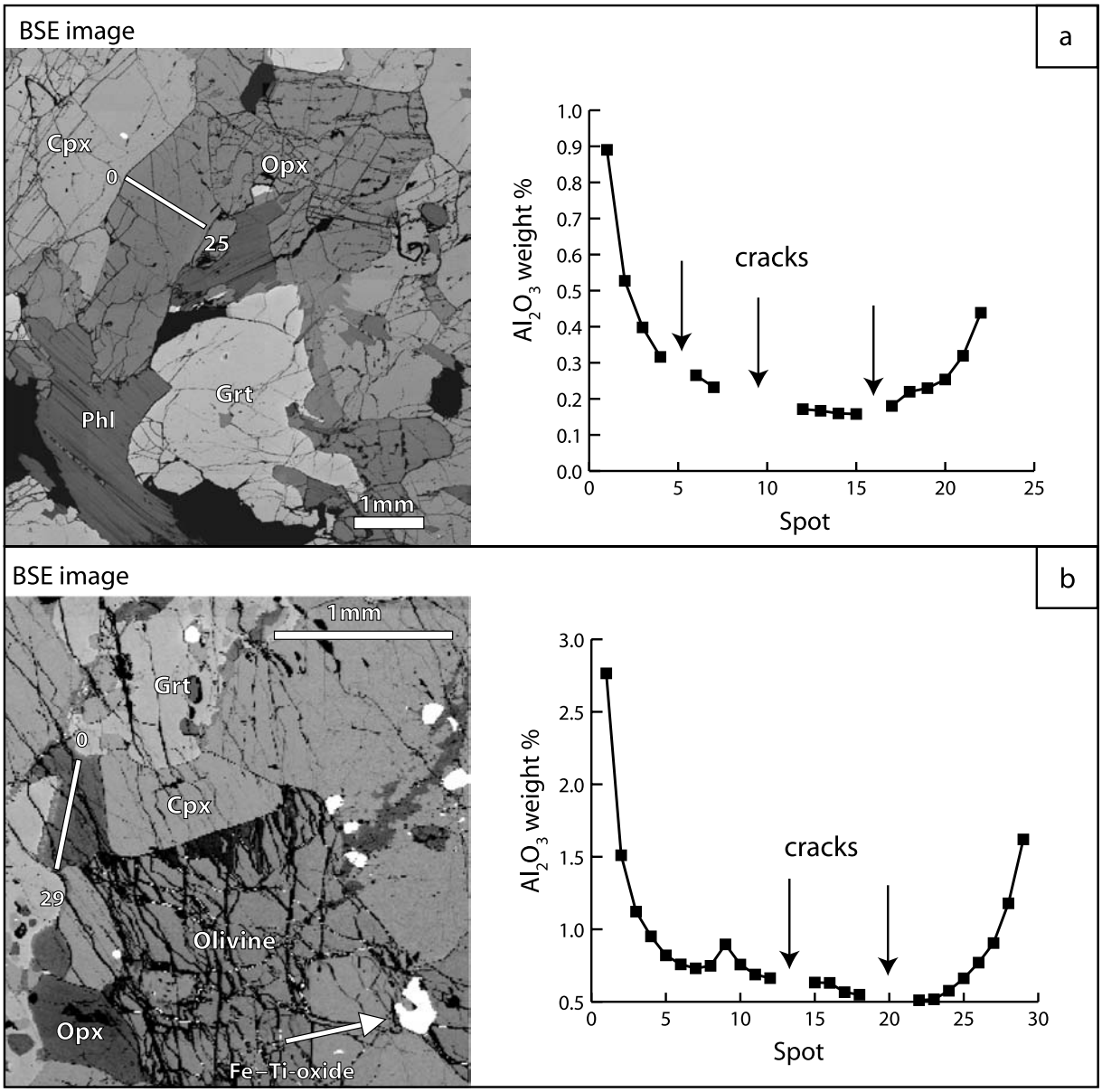

Fig. 4. (a) Back-scatter electron image from a selected part in a thin section of the garnet websterite vein (a) sample 6 and (b) sample 8. The lines show location of the Al_2O_3 abundance profile (diagram to the right) along the orthopyroxene grain. Also visible are the Fe–Ti oxides characteristic of the Fe–Ti type garnet peridotites

Geothermobarometry

Peak *P–T* values were obtained using the lowest Al_2O_3 contents in cores of orthopyroxene grains in combination with core values of adjacent, chemically unzoned minerals (Table 1). The pressure–temperature conditions listed in Table 2 were obtained by combining the various thermometers reported in the method section with the *Brey* and *Köhler* (1990) barometer. The thermometers have also been

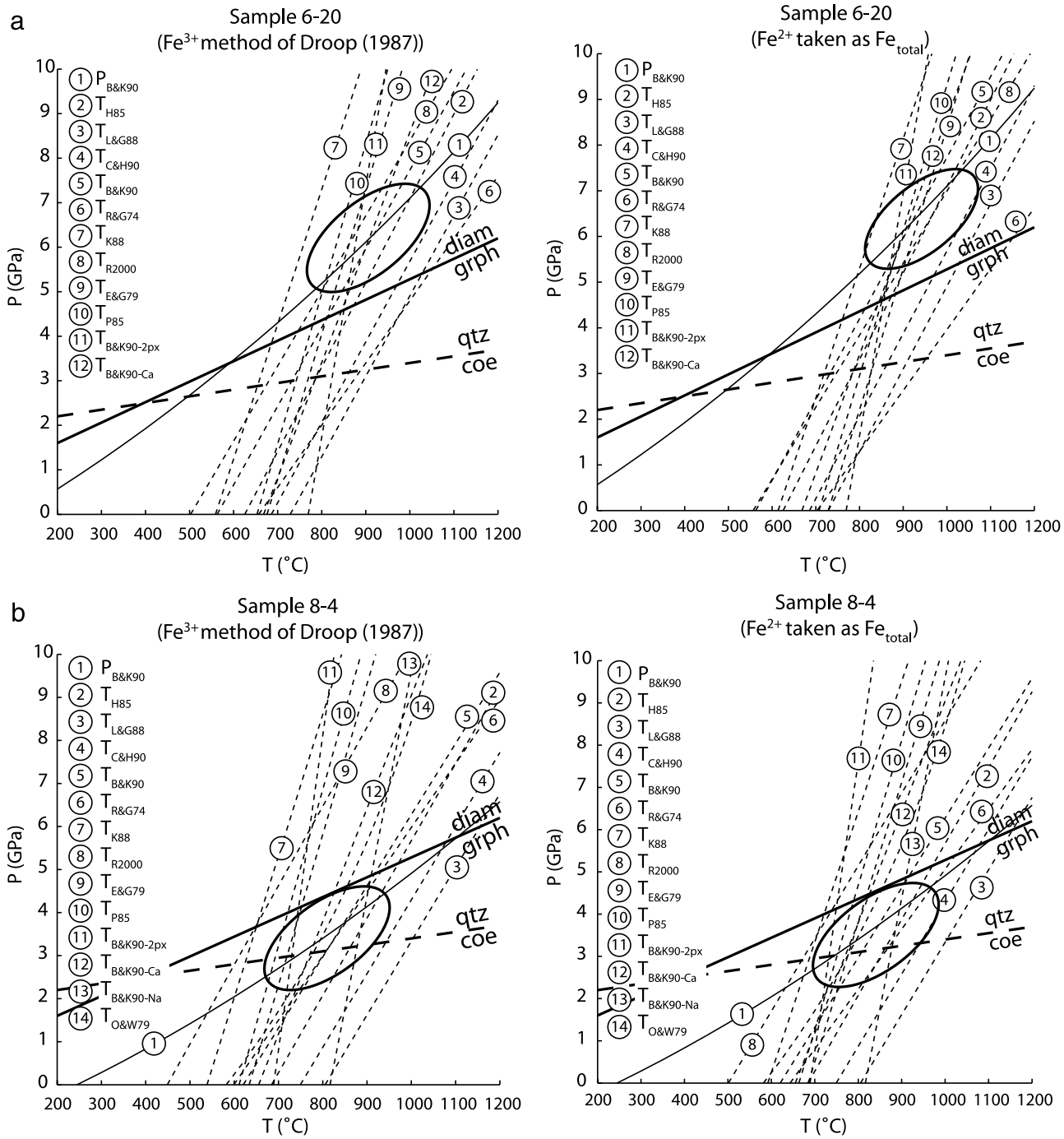

Fig. 5. Geothermobarometry results for selected samples 6 (garnet websterite vein) and 8 (garnet peridotite body). Diamond-graphite equilibrium line from *Bundy* (1980), coesite-quartz equilibrium line from *Hemingway* et al. (1998)

combined with other barometers (e.g. $P_{H\&G82}$, P_{H84} and $P_{N\&G85}$), however, the obtained geothermobarometric results were not significantly different. A wide range of *P–T* estimates can thus be obtained using various combinations of differ-

ent geothermobarometers. It is, however, beyond the scope of this paper to evaluate which thermometers and barometers represent the most reliable results. For this we refer the reader to *Carswell* and *Harley* (1990), *Krogh* and *Carswell* (1995) and *Ravna* and *Paquin* (2003).

Our results, shown in Fig. 5 and listed in Table 2, demonstrate that for the garnet-websterite vein (sample 6) most calculated *P–T* conditions are well above the graphite-diamond phase boundary line (see Fig. 5a and b), in agreement with the presence of micro-diamond (*Vrijmoed* et al., in prep.). These observations provide unambiguous evidence that the cross-cutting garnet websterite vein records UHPM conditions within the diamond stability field. We conclude that 5.5 GPa and 800 °C is representative of the formation conditions of the UHP mineralogy in the veins.

In contrast, most geothermobarometric results from the peridotite body (sample 8) record UHPM conditions restricted to the coesite field. The data in Table 2 imply that the last recorded equilibration of the main body occurred at 3.4 GPa and 800 °C. Although most of the latter results still define UHPM conditions, we interpret the lower *P–T* estimates in the peridotite body compared to the veins, to be due to post-peak metamorphic aluminium diffusion effects in orthopyroxene related to exhumation. These pressure estimates for the peridotite body are therefore regarded to represent minimum pressure conditions. Our geothermobarometric results thus support an expansion of the northernmost UHP terrain in the WGR in Norway at least 25 km northeastwards.

The garnet websterite preserves higher equilibrium conditions than the peridotite. Our explanation for this apparent difference in metamorphic grade is that the garnet websterite veins have a 2–10 times larger grain size than the surrounding Fe–Ti type peridotite body resulting in a higher effective closure temperature for the Sm–Nd isotope system. More work is required to fully explain the apparent pressure difference between UHP mineralogy of the websterite veins and peridotite body.

Isotope geochemistry

Sm–Nd

Isotopic results are reported in Table 3. Sm–Nd garnet-clinopyroxene isochrons of samples 6 (garnet websterite vein) and 8 (garnet peridotite body) are presented in Fig. 7. The two Sm–Nd isochron ages of 381 ± 6 Ma and 393 ± 3 Ma are significantly different but define roughly similar initial $^{143}Nd/^{144}Nd$ isotope ratios of 0.51171 ± 0.00002 and 0.51195 ± 0.00001 respectively. These ratios equate to ε_{Nd} values of -8.5 and -3.6 respectively. These ages are significantly younger than the time proposed for peak metamorphism in the Caledonian Orogeny (*Hacker* et al., 2001; *Carswell* et al., 2003b). Nd model ages of the whole rocks are summarised in Fig. 8 and Table 3. Initial $^{143}Nd/^{144}Nd$ ratios at 400 Ma are between 0.51167 and 0.51191, comparable to the $^{143}Nd/^{144}Nd$ values of the two mineral isochrons (Fig. 7a and b). There is, however, no distinction between the initial ratios of the whole rock samples of the websterite vein and peridotite body. Below we will use the isotope geochemistry of the peridotites to examine the petrogenesis of these rocks to assess the geological significance of the mineral and model ages and discuss the petrogenesis of the Svartberget peridotite body.

Sr–Nd isotopes

Rb–Sr isotope analyses of leached minerals from the peridotite body, a cross-cutting garnet websterite vein and two ‘‘country-rock’’ eclogite lenses were conducted

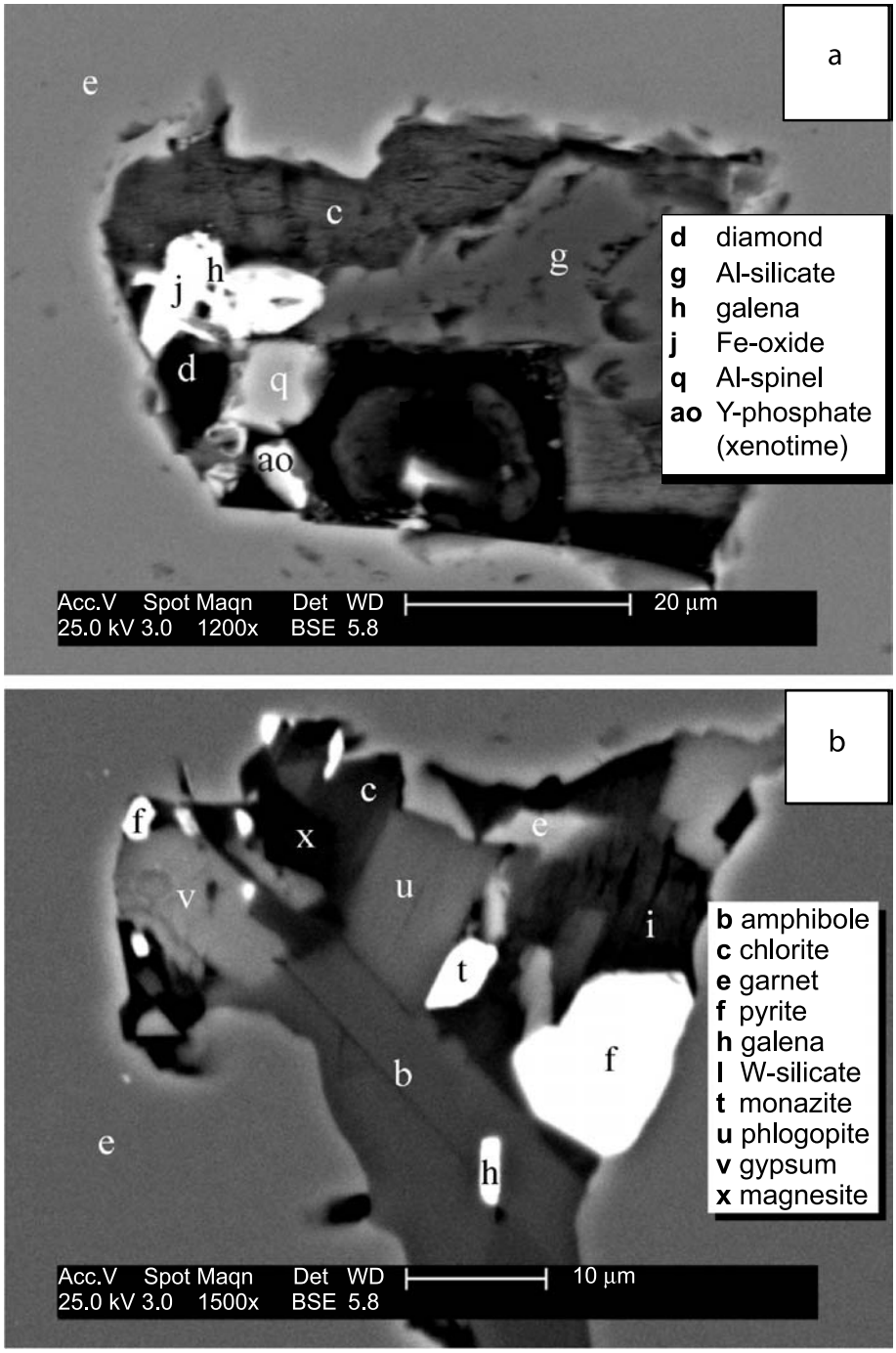

Fig. 6. Polyphase solid inclusions in garnets of the websterite (sample 6) showing a variety of minerals in a single inclusion assemblage, with microdiamond in Fig. (a)

to constrain the potential origin of the fluids that produced the polyphase solid inclusions. Sr–Nd isotope ratios are plotted at 400 Ma in Fig. 7d and show that $^{87}Sr/^{86}Sr$ ratios are extremely high for the garnet peridotite and even higher for the garnet websterite vein minerals compared to the eclogite boudins occurring in the area (sample 79 and 99) and expected mantle compositions at that time. Rb concentrations are very low so that the radiogenic Sr cannot be a consequence of Rb decay or an incorrect calculation of the initial Sr isotope ratios. The high Sr ratios for the garnet websterites implies that they contain a component originating from the crust. High $^{87}Sr/^{86}Sr$ ratios unsupported by Rb have previously been reported in the WGR and were explained by Rb loss associated with high temperature metamorphism (*Griffin* and *Brueckner*, 1985; *Austrheim* et al., 2003). However, the presence of the polyphase solid inclusions strongly suggests that infiltrating C–O–H rich melts from external (felsic) sources transported radiogenic Sr into the peridotites to form the websterites and garnetites.

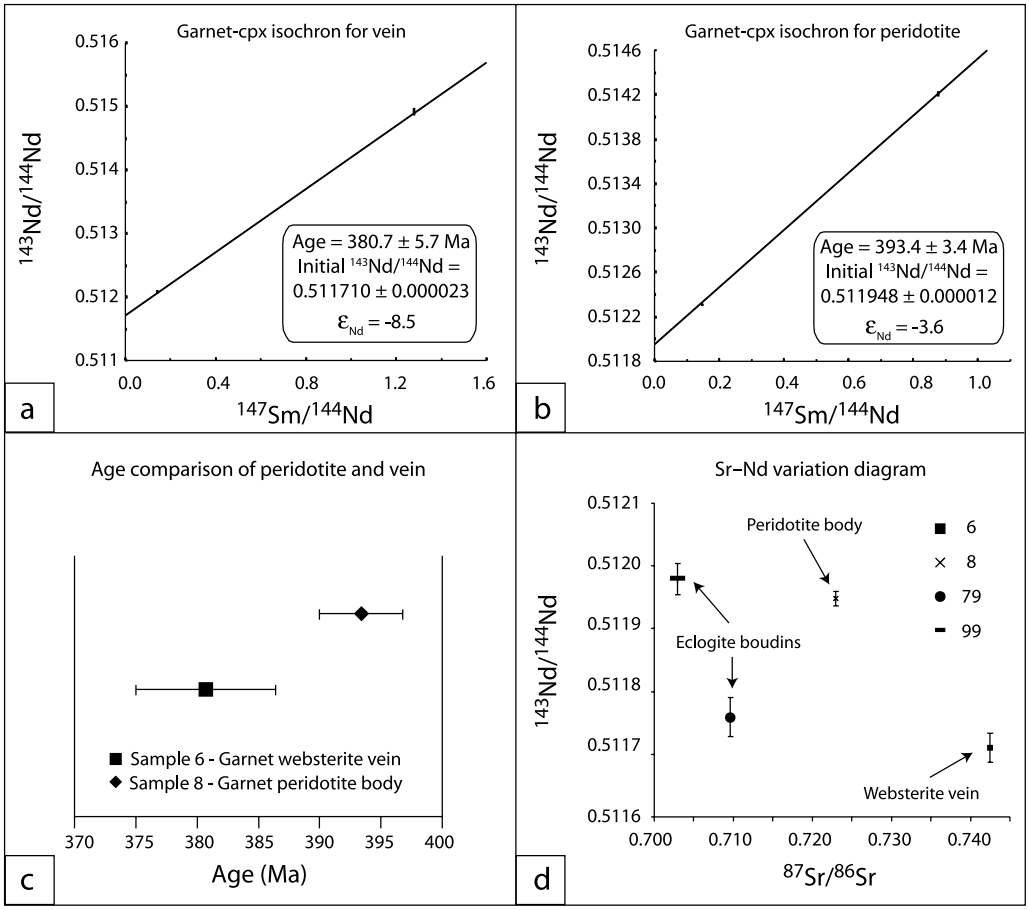

Fig. 7. (a) Sm–Nd grt-cpx isochron of garnet websterite vein (sample 6) and (b) Sm–Nd grt-cpx isochron of garnet peridotite (sample 8). (c) Comparison diagram of the two ages (a) and (b) with their error bars. (d) Sr–Nd isotope ratios diagram of the garnet websterite (sample 6) the garnet peridotite (sample 8) and two "country-rock" eclogites from our area (sample 79 and 99, see Fig. 2)

The mineral isochron ages (380–395 Ma) are significantly younger than the generally accepted ~400 Ma age for UHPM in the WGR (*Hacker* et al., 2001; *Carswell* et al., 2003a). Sm–Nd isotope dating using 2-points isochrons will provide geologically unrealistic ages if garnet or clinopyroxene contain phases of different paragenesis that contain a significant proportion of the Sm and or Nd. Although mineral separates were extremely carefully hand-picked and subjected to leaching, it is well known that minor phases can remain undetected (*Thöni*, 2002). In the case of the Svartberget body, there are polyphase solid inclusions of among other minerals monazite (Fig. 6b), which have high REE concentrations. The presence of such phases may have led to mineral ages that are too young.

The mineral isochrons record the end of diffusion of Sm and Nd between the constituent minerals in the rock. The closure temperature for the Sm–Nd system depends on many factors such as composition, grain-size, cooling rate, diffusion parameters (*Ganguly* et al., 1998; *Van Orman* et al., 2002). Current values for some of these parameters are experimentally determined on gem quality phases and are therefore subject to geological uncertainty. Our best estimate of the closure temperature, derived using the diffusion program of *Ganguly* and *Tirone*, 1999, yielded temperatures around 750–800 °C. Considering the fact that the temperature of the amphibolite facies metamorphism was around 750–800 °C (*Cuthbert* et al., 2000), and assuming that the closure temperatures are about 750–800 °C, it is probable that we have dated closure of the Sm–Nd system during amphibolite facies conditions.

Krogh et al. (2003) reported 415 Ma zircon age from eclogites from the Averøya area northeast of the area investigated in this study and 385 Ma for zircons from pegmatites in amphibolite facies boudin necks in the same area. The Sm–Nd mineral cooling ages from the garnet peridotite body may therefore also be recording a thermal event associated with pegmatite activity.

The garnet websterite (sample 6) was sampled within 1 m of low pressure pegmatite veins post-dating the main body and the garnet websterite veins. Nevertheless, this Sm–Nd isochron age of 380 Ma gives an indication that the (UHP) metamorphic event that formed the garnet–websterite mineralogy was Scandian in age and not Proterozoic.

We conclude that there are several potential explanations for the fact that the Sm–Nd mineral ages are younger than the timing of Caledonian peak metamorphic conditions; (1) The obtained ages may record cooling following amphibolite facies metamorphism; (2) The minerals may have been affected thermally by late pegmatite veins; (3) It is possible that REE-rich minor phases, that retain a pre-metamorphic history, are included in the garnet separates. Continued research is underway to provide a full explanation of the *P–T-t* evolution of the Svartberget garnet peridotite body.

Geological history

The data presented in this study allows part of the geological history of the UHP Fe–Ti peridotite-websterite body to be determined. The mineralogy and petrology of the Svartberget garnet peridotite body closely resembles other Fe–Ti type peridotites in the WGR (*Schmidt*, 1963; *Carswell* et al., 1983; *Jamtveit*, 1987a, b).

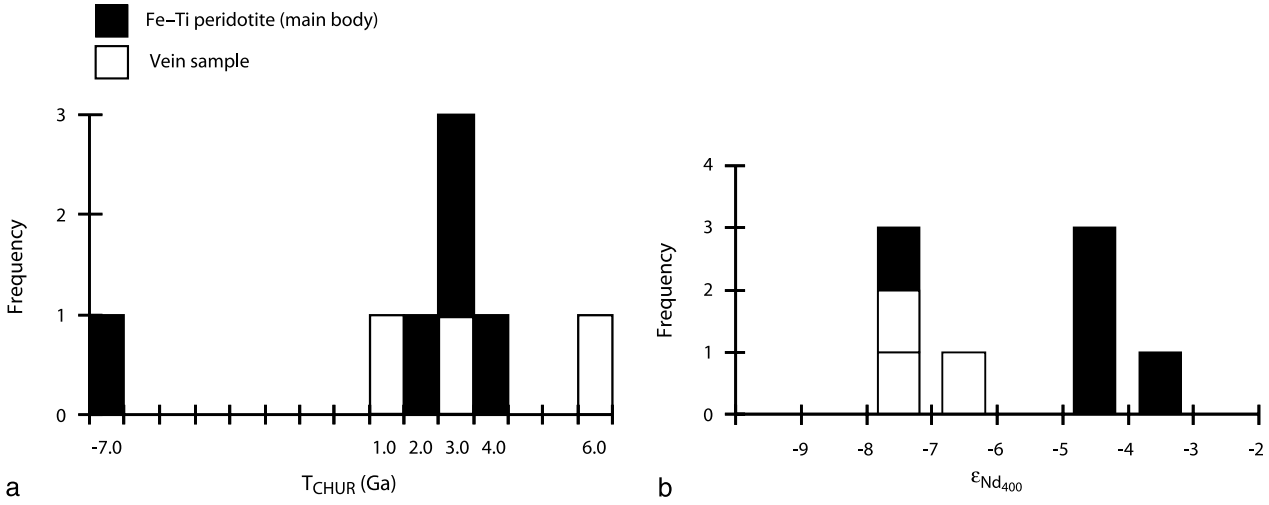

Fig. 8. Diagrams of (a) Sm–Nd T_{CHUR} model ages and (b) ε_{Nd} values at 400 Ma BP from all samples

These rocks are believed to be formed from Proterozoic cumulates in the lower crust. The initial ratio of the peridotite mineral isochron (ε_{Nd} of -3.6) suggests that these rocks had a pre-history of $\sim$1 Ga, consistent with a Proterozoic age. Nd model ages have a large spread, but most of them indicate a Proterozoic (1500–2500 Ma) age, which is in line with the other Fe–Ti type garnet peridotites.

We believe there are three factors that contribute to the wide spread in Nd model ages (Fig. 8). Fractionation of garnet assemblages from a melt/fluid will lead to a marked fractionation of Sm/Nd leading to decoupling of the parent daughter ratio and the time integrated Nd isotope ratio. The significance of the Nd model ages of the websterite–garnetite assemblages with very variable garnet contents (5–100%), is therefore difficult to assess without detailed knowledge of their petrogenesis. In addition, the metamorphic formation of relatively garnet-rich and -poor peridotites will also cause re-distribution of REE and potentially disruption of Nd model ages.

The radiogenic Sr isotope ratios, coupled with the polyphase inclusions, suggest that the websterites were formed by volatile-rich melts that had interacted extensively with the continental crust. These melts would transport Nd derived from the Proterozoic crust leading to apparent Proterozoic ages and due to garnet fractionation a large scatter of the Nd model ages. We therefore follow previous workers in interpreting the Fe–Ti garnet peridotites as lower crustal cumulates formed in layered mafic igneous intrusions during the Proterozoic (*Schmidt*, 1963; *Mørk*, 1985a, b; *Jamtveit*, 1987a, b).

We consider the fact that the polyphase solid inclusions are randomly located in garnet to be highly significant. The simplest interpretation is that inclusions crystallised synchronously with the garnet-websterites and garnetites under diamond facies UHP conditions. Alternatively they may have been introduced to existing minerals during UHP garnet growth. However, it is difficult to envisage how metamorphic reactions and mineral recrystallisation would not lead to the formation of inclusion trails. Therefore our favoured geological evolution of the Svartberget garnet peridotite body began with formation in the Proterozoic. During Scandian

times volatile-rich melts/fluids infiltrated the garnet peridotite body during diamond facies UHPM forming garnet websterite/garnetite veins that trapped fluids that are preserved as polyphase solid inclusions. The melts were most likely C–O–H-rich ''fluids'' that originate from crustal sources carrying large ion lithophile and highly incompatible elements (Rb, Th, LREE etc). We speculate that fracturing and vein emplacement were the result of local high fluid pressure caused by the dehydration of the Baltic plate during subduction.

Tectonic implications

The data presented in this paper suggest that the northern UHP domain in the WGR can be extended approximately 25 km northeastwards. Therefore the northern UHP domain in the WGR has a length of ~75 km. The other two UHP domains in WGR are of comparable size. Although the three UHP domains are arbitrary grouping of UHPM rocks in the WGR of Norway (Fig. 1) the following question arises: Do they represent one individual large domain or several small sub domains. Resolution of this question has important implication for the processes responsible for the exhumation of the UHP domains. In the case of a single large UHP domain, the domain might have returned to the surface buoyancy driven as a large coherent nappe (*Ernst*, 1973; *Chemenda* et al., 1995; *Brueckner* and *Van Roermund*, 2004). But in the case of small sub domains, the domains might have returned to the surface as small slivers, separated by thrusts. In this latter case, variation in exhumation and subduction rates and residence time may produce distinct *P–T-t* trajectories in the individual domains, while a coherent nappe will produce a coherent set of *P–T-t* trajectories.

The present study establishes that the size and extent of the northern UHP domain is not completely known. Therefore more detailed mapping and subsequent *P–T* and geochemical analysis on neighbouring areas is required to reveal the size and inter-relationships of the UHP domains in the WGR.

A major implication of this work is that the paragneissic basement of the WGR, regionally referred to as the Ulla Gneiss, has undergone UHPM (diamond grade). This conclusion is in strong contrast with the work of *Terry* and *Robinson* (2004) at the island of Fjørtoft. The latter authors recognised a major tectonic break on Fjørtoft between a northern UHP (diamond grade) segment and a southern Ulla-Gneiss-related terrane, metamorphosed at 2.0 GPa and 750–800 °C. The present study indicates that the Ulla-Gneiss related unit was also metamorphosed at UHPM (diamond grade) conditions, leaving no evidence for a major tectonic break. Such a conclusion is also in agreement with the work of *Carswell* et al. (2006).

Conclusions

Lithological and structural field data combined with isotope geochemistry and geothermobarometry in the Bud-Tornes region of the WGR have led us to the following conclusions:

A new occurrence of Fe–Ti type garnet peridotite, named Svartberget, lies along strike with other Fe–Ti type garnet peridotites. The occurrence of diamond and *P–T* estimates establish that the rocks have been at diamond grade UHP conditions.

Consequently, the northern UHP domain in the Western Gneiss Region in Norway can be extended approximately 25 km towards the northeast.

The Svartberget peridotite body was cross-cut by a network of garnet-websterites and garnetites. Textural and mineralogical evidence from polyphase solid inclusions, Sm–Nd whole rock and Sr-isotope data suggest that crustal derived C–O–H rich melts/fluids infiltrated the Svartberget body, probably during Caledonian subduction, forming a network of garnet websterite and garnetite veins with pronounced preferred orientations.

Young Caledonian Sm–Nd garnet-clinopyroxene ages are either the result of REE-rich micro-inclusions that cannot be removed by leaching, or they represent a cooling age somewhat later than the UHPM, possibly the result of influx of pegmatite veins. The mineral ages do, however, demonstrate that the last metamorphic equilibration was associated with the Caledonian Orogeny. The initial ratio of the garnet peridotite mineral isochron implies a Proterozoic origin. However, the large range in Nd model ages from the peridotite body can be explained by the involvement of crustal derived (high $^{87}Sr/^{86}Sr$) C–O–H bearing melts/fluids, and or by garnet fractionation that disrupted the Sm–Nd isotope systematics.

The present study shows that the size and extent of the northern UHP domain is not completely known. More detailed mapping and subsequent *P–T* and geochemical analysis on neighbouring areas is required to reveal the size and inter-relationships of the UHP domains in the WGR. This work is required to better understand the exhumation mechanisms of the UHP rocks.

Acknowledgements

We would like to thank the Faculty of Earth and Life Sciences at the VU in Amsterdam and the Faculty of Earth Sciences at the Utrecht University for providing the funding for this project and access to the laboratories at the two universities. The fieldwork was partly funded by a grant from the Dittmer fund of the VU. We thank Håkon Austrheim and Muriel Erambert at the University of Oslo for useful discussions and help on geothermobarometry. Two highly constructive reviews by Erling Ravna and Simon Cuthbert and editorial handling by Aberra Mogessie significantly improved the structure of this manuscript.

References

Andersen TB (1998) Extensional tectonics in the Caledonides of southern Norway, an overview. Tectonophysics 285: 333–351

Austrheim H, Corfu F, Bryhni I, Andersen TB (2003) The Proterozoic Hustad igneous complex: a low strain enclave with a key to the history of the Western Gneiss Region of Norway. Precambrian Res 120: 149–175

Brey GP, Köhler T (1990) Geothermobarometry in Four-phase Lherzolites. II. New Thermobarometers, and Practical Assessment of Existing Thermobarometers. J Petrol 31: 1353–1378

Brueckner HK, Van Roermund HLM (2004) Dunk tectonics: a multiple subduction/education model for the evolution of the Scandinavian Caledonides. Tectonics 23, DOI: TC2004, 10.1029/2003TC001502

Bryhni I (1989) Status of the supracrustal rocks in the Western Gneiss Region, S. Norway. In: *Gayer RA* (ed) The Caledonide Geology of Scandinavia. Graham & Trotman, pp 221–228

Bryhni I, Austrheim H, Solli A (1989) HUSTAD berggrunnskart 1220 1 Norges Geologiske Undersøkelse, Trondheim, foreløpig utgave

Bryhni I, Sturt BA (1985) Caledonides of southwestern Norway. In: *Gee DG, Sturt BA* (eds) The Caledonide Orogen; Scandinavia and related areas, vol 1. John Wiley & Sons, Chichester, United Kingdom, pp 89–107

Bundy FP (1980) The P, T phase and reaction diagram for elemental carbon. J Geophys Res 85: 6930–6936

Carswell DA, Brueckner HK, Cuthbert SJ, Mehta K, O'Brien PJ (2003a) The timing of stabilisation and the exhumation rate for ultra-high pressure rocks in the Western Gneiss Region of Norway. J Metamorph Geol 21: 601–612

Carswell DA, Harley SL (1990) Mineral barometry and thermometry. In: *Carswell DA* (ed) Eclogite facies rocks. Blackie, Glasgow, pp 83–110

Carswell DA, Harvey MA (1982) The intrusive history and tectono-metamorphic evolution of the Basal Gneiss Complex in the Moldefjord region, W. Norway. J Geol Soc London 139: 368–368

Carswell DA, Harvey MA, Al-Samman A (1983) The petrogenesis of contrasting Fe–Ti and Mg–Cr garnet peridotite types in the high-grade gneiss complex of Western Norway. B Mineral 106: 727–750

Carswell DA, Tucker RD, O'Brien PJ, Krogh TE (2003b) Coesite micro-inclusions and the U/Pb age of zircons from the Hareidland eclogite in the Western Gneiss Region of Norway. Lithos 67: 181–190

Carswell DA, Van Roermund HLM (2005) On multi-phase mineral inclusions associated with microdiamond formation in mantle-derived peridotite lens at Bardane on Fjortoft, west Norway. Eur J Mineral 17: 31–42

Carswell DA, Van Roermund HLM, Wiggers de Vries D (2006) Scandian ultra-high pressure metamorphism of Proterozoic Basement rocks on Fjørtoft and Otrøy in the Western Gneiss Region of Norway. Int Geol Rev Accepted

Chemenda AI, Mattauer M, Malavieille J, Bokun AN (1995) A mechanism for syn-collisional rock exhumation and associated normal faulting – results from physical modeling. Earth Planet Sc Lett 132: 225–232

Cuthbert SJ, Carswell DA, Krogh-Ravna EJ, Wain A (2000) Eclogites and eclogites in the Western Gneiss Region, Norwegian Caledonides. Lithos 52: 165–195

Dobrzhinetskaya LF, Eide EA, Larsen RB, Sturt BA, Tronnes RG, Smith DC, Taylor WR, Posukhova TV (1995) Microdiamond in high-grade metamorphic rocks of the Western Gneiss Region, Norway. Geology 23: 597–600

Dodson MH (1973) Closure Temperature in Cooling Geochronological and Petrological Systems. Contrib Mineral Petrol 40: 259–274

Droop GTR (1987) A general equation for estimating Fe^{3+} concentrations in ferromagnesian silicates and oxides from microprobe analyses, using stoichiometric criteria. Mineralog Mag 51: 431–435

Ellis DJ, Green DH (1979) Experimental-study of the effect of Ca upon garnet-clinopyroxene Fe–Mg exchange equilibria. Contrib Mineral Petrol 71: 13–22

Ernst WG (1973) Interpretative synthesis of metamorphism in Alps. Geol Soc Am Bull 84: 2053–2078

Ganguly J, Tirone M (1999) Diffusion closure temperature and age of a mineral with arbitrary extent of diffusion: theoretical formulation and applications. Earth Planet Sc Lett 170: 131–140

Ganguly J, Tirone M, Hervig RL (1998) Diffusion kinetics of samarium and neodymium in garnet, and a method for determining cooling rates of rocks. Science 281: 805–807

Griffin WL, Austrheim H, Brastad K, Bryhni I, Krill AG, Krogh EJ, Mørk MBE, Qvale H, Torudbakken B (1985) High-pressure metamorphism in the Scandinavian Caledonides. In: *Gee DG, Sturt BA* (eds) The Caledonide Orogen; Scandinavia and related areas, vol 2. John Wiley & Sons, Chichester, United Kingdom, pp 783–801

Griffin WL, Brueckner HK (1985) Ree, Rb–Sr and Sm–Nd Studies of Norwegian Eclogites. Chem Geol 52: 249–271

Griselin M (2001) Geochemical and isotopic study of the Xigaze and Luabusa ophiolite massifs (Yarlung Zangbo Suture Zone, Southern Tibet): implications for partial melting and dynamic evolution of the Neo-Tethys Ocean Unpubl. Ph.D. Thesis Vrije Universiteit, Amsterdam, 216 p

Griselin M, van Belle JC, Pomies C, Vroon PZ, van Soest MC, Davies GR (2001) An improved chromatographic separation technique of Nd with application to NdO^+ isotope analysis. Chem Geol 172: 347–359

Hacker B, Root D, Walsh E, Young D, Mattinson J (2001) Recent progress on the Norwegian HP-UHP eclogites. Abstract to UHPM Workshop at Waseda University, Japan 4B06: 174

Harley SL (1984a) An experimental study of the partitioning of Fe and Mg between garnet and orthopyroxene. Contrib Mineral Petrol 86: 359–373

Harley SL (1984b) The Solubility of Alumina in Orthopyroxene Coexisting with Garnet in $FeO–MgO–Al_2O_3–SiO_2$ and $CaO–FeO–MgO–Al_2O_3–SiO_2$. J Petrol 25: 665–696

Harley SL, Green DH (1982) Garnet orthopyroxene barometry for granulites and peridotites. Nature 300: 697–701

Harvey MA (1983) A geochemical and Rb–Sr study of the Proterozoic augen orthogneisses on the Molde peninsula, west Norway. Lithos 16: 325–338

Hemingway BS, Bohlen SR, Hankins WB, Westrum EF, Kuskov OL (1998) Heat capacity and thermodynamic properties for coesite and jadeite, reexamination of the quartz-coesite equilibrium boundary. Am Mineral 83: 409–418

Hermann J (2003) Experimental evidence for diamond-facies metamorphism in the Dora-Maira massif. Lithos 70: 163–182

Jamtveit B (1987a) Magmatic and metamorphic controls on chemical variations within the Eiksunddal eclogite complex, Sunnmore, Western Norway. Lithos 20: 369–389

Jamtveit B (1987b) Metamorphic evolution of the Eiksunddal eclogite complex – Western Norway, and some tectonic implications. Contrib Mineral Petrol 95: 82–99

Krabbendam M, Dewey JF (1998) Exhumation of UHP rocks by transtension in the Western Gneiss Region, Scandinavian Caledonides. Geol Soc Spec Publ 135: 159–181

Krill AG (1985) Relationships between the Western Gneiss Region and the Trondheim region; stockwerk-tectonics reconsidered. In: *Gee DG, Sturt BA* (eds) The Caledonide Orogen; Scandinavia and related areas, vol 1. John Wiley & Sons, Chichester, United Kingdom, pp 475–483

Krogh EJ (1977) Evidence of Precambrian continent–continent collision in Western Norway. Nature 267: 17–19

Krogh EJ (1988) The garnet-clinopyroxene Fe–Mg geothermometer – a reinterpretation of existing experimental data. Contrib Mineral Petrol 99: 44–48

Krogh EJ, Carswell DA (1995) HP and UHP Eclogites and Garnet Peridotites in the Scandinavian Caledonides. In: *Coleman RG, Wang X* (eds) Ultrahigh Pressure Metamorphism. Cambridge University Press, pp 244–298

Krogh T, Robinson P, Terry MP (2003) Precise U–Pb zircon ages define 18 and 19 m.y. Subduction to uplift intervals in the Averøya-Nordøyane area, Western Gneiss Region. NGU-report 2003-055: 71–72

Lee HY, Ganguly J (1988) Equilibrium compositions of coexisting garnet and orthopyroxene – experimental determinations in the system FeO–MgO–Al_2O_3–SiO_2, and Applications. J Petrol 29: 93–113

Mørk MBE (1985a) A gabbro to eclogite transition on Flemsøy, Sunnmore, Western Norway. Chem Geol 50: 283–310

Mørk MBE (1985b) Incomplete high P–T metamorphic transitions within the Kvamsøy pyroxenite complex, West Norway – a case-study of disequilibrium. J Metamorph Geol 3: 245–264

Nickel KG, Green DH (1985) Empirical geothermobarometry for garnet peridotites and implications for the nature of the lithosphere, kimberlites and diamonds. Earth Planet Sc Lett 73: 158–170

O'Neill HSC (1980) Correction. Contrib Mineral Petrol 72: 337

O'Neill HSC, Wood BJ (1979) Experimental-Study of Fe–Mg Partitioning between garnet and olivine and its calibration as a geothermometer. Contrib Mineral Petrol 70: 59–70

Powell R (1985) Regression diagnostics and robust regression in geothermometer geobarometer calibration – the garnet clinopyroxene geothermometer revisited. J Metamorph Geol 3: 231–243

Råheim A, Green DH (1974) Experimental determination of the temperature and pressure dependence of the Fe–Mg partition coefficient for coexisting garnet and clinopyroxene. Contrib Mineral Petrol 48: 179–203

Ravna EJK (2000) The garnet-clinopyroxene Fe^{2+}–Mg geothermometer: an updated calibration. J Metamorph Geol 18: 211–219

Ravna EJK, Paquin J (2003) Thermobarometric methodologies applicable to eclogites and garnet ultrabasites. In: *Carswell DA, Compagnoni R* (eds) Ultrahigh pressure metamorphism, vol. EMU Notes in Mineralogy 5, pp 229–259

Roberts D (2003) The Scandinavian Caledonides: event chronology, palaeogeographic settings and likely, modern analogues. Tectonophysics 365: 283–299

Robinson P (1995) Extension of Trollheimen tectono-stratigraphic sequence in deep synclines near Molde and Brattvåg, Western Gneiss Region, Southern Norway. Norsk Geol Tidsskr 75: 181–197

Root DB, Hacker BR, Gans PB, Ducea MN, Eide EA, Mosenfelder JL (2005) Discrete ultrahigh-pressure domains in the Western Gneiss Region, Norway: implications for formation and exhumation. J Metamorph Geol 23: 45–61

Sambridge M, Lambert DD (1997) Propagating errors in decay equations: examples from the Re–Os isotopic system. Geochim Cosmochim Acta 61: 3019–3024

Schmidt HH (1963) Petrology and structure of the Eiksundal Eclogite Complex, Hareidlandet, Sunnmore, Norway Unpubl. Ph.D. Thesis Harvard University, U.S.A., 323 p

Seranne M (1992) Late Paleozoic Kinematics of the More-Trondelag Fault Zone and adjacent areas, central Norway. Norsk Geol Tidsskr 72: 141–158

Smith DC (1984) Coesite in clinopyroxene in the Caledonides and its implications for geodynamics. Nature 310: 641–644

Stalder P, Ulmer P, Thompson AB, Gunther D (2000) Experimental approach to constrain second critical end points in fluid/silicate systems: near-solidus fluids and melts in the system albite-H_2O. Am Mineral 85: 68–77

Terry MP, Robinson P (2003) Evolution of amphibolite-facies structural features and boundary conditions for deformation during exhumation of high- and ultrahigh-pressure rocks, Nordoyane, Western Gneiss Region, Norway. Tectonics 22: 1036, DOI: 10.1029/2001 TC001349

Terry MP, Robinson P (2004) Geometry of eclogite-facies structural features: implications for production and exhumation of ultrahigh-pressure and high-pressure rocks, Western Gneiss Region, Norway. Tectonics 23: TC2001, DOI: 10.1029/2002TC001401

Terry MP, Robinson P, Ravna EJK (2000) Kyanite eclogite thermobarometry and evidence for thrusting of UHP over HP metamorphic rocks, Nordøyane, Western Gneiss Region, Norway. Am Mineral 85: 1637–1650

Thöni M (2002) Sm–Nd isotope systematics in garnet from different lithologies (Eastern Alps): age results, and an evaluation of potential problems for garnet Sm–Nd chronometry. Chem Geol 185: 255–281

Torsvik TH, Smethurst MA, Meert JG, Van der Voo R, McKerrow WS, Brasier MD, Sturt BA, Walderhaug HJ (1996) Continental break-up and collision in the Neoproterozoic and Palaeozoic – a tale of Baltica and Laurentia. Earth-Sci Rev 40: 229–258

Tveten E, Lutro O, Thornes T (1998) Geologisk kart over Norge, berggrunnskart, ÅLESUND 1:250.000 Norges geologiske undersøkelse, Geological map

Van Orman JA, Grove TL, Shimizu N, Layne GD (2002) Rare earth element diffusion in a natural pyrope single crystal at 2.8 GPa. Contrib Mineral Petrol 142: 416–424

Van Roermund HLM, Carswell DA, Drury MR, Heijboer TC (2002) Microdiamonds in a megacrystic garnet websterite pod from Bardane on the island of Fjørtoft, western Norway: evidence for diamond formation in mantle rocks during deep continental subduction. Geology 30: 959–962

Van Roermund HLM, Spengler D, Wiggers de Vries D (2005) Evidence for ultra-high pressure (UHP) metamorphism within Proterozoic basement rocks on Otrøy, Western Gneiss Region, Norway. Mitt Osterr Miner Ges 150: 159

Van Straaten B, Wiggers de Vries D, Van Roermund HLM, Drury M (2003) A structural, metamorphic and geochronological study of eclogites and country rock gneisses from Otrøy (Moldefjord), WGR, Norway. Norg Geol Unders Report 2003.055: 155–156

Vrijmoed JC, Smith DC, Van Roermund HLM (In preparation) A new in-situ microdiamond locality in the Scandinavian Caledonides: Svartberget

Wells PRA (1977) Pyroxene thermometry in simple and complex systems. Contrib Mineral Petrol 62: 129–139

Authors' addresses: *J. C. Vrijmoed* (corresponding author; e-mail: j.c.vrijmoed@fys.uio.no), *G. R. Davies*, Petrology Department, Faculty of Earth and Life Science, Free University Amsterdam, De Boelelaan 1085, Amsterdam, the Netherlands; *H. L. M. Van Roermund*, Structural Geology Group, Faculty of Earth Sciences, Utrecht University, Budapestlann 4, 3508 TA, Utrecht, the Netherlands

Verleger: Springer-Verlag GmbH, Sachsenplatz 4–6, 1201 Wien, Austria – Herausgeber: Prof. Dr. J. G. Raith, Department Angewandte Geowissenschaften und Geophysik, Lehrstuhl für Mineralogie und Petrologie, Peter-Tunner-Straße 5, 8700 Leoben, Austria – Redaktion: Peter-Tunner-Straße 5, 8700 Leoben, Austria – Satz und Umbruch: Thomson Press (India) Ltd., Chennai; Offsetdruck: Novographic Druck G.m.b.H., Sagedergasse 29, 1120 Wien, Austria – Verlagsort: Wien – Herstellungsort: Wien – Printed in Austria.